Rheological Behavior of Aqueous Polyurethane Dispersions: Effects of Solid Content, Degree of Neutralization, Chain Extension, and Temperature

Samy A. Madbouly,† Joshua U. Otaigbe,* Ajaya K. Nanda, and Douglas A. Wicks

School of Polymers and High Performance Materials, The University of Southern Mississippi, Hattiesburg, Mississippi 39406

Received March 3, 2005

ABSTRACT: Rheological behavior of waterborne polyurethane dispersions was investigated with small-amplitude oscillatory shear flow experiments over wide ranges of concentration, degree of neutralization, chain extension, and temperatures to accelerate efforts to understand their film formation characteristics. The rheological properties of these environmentally friendly dispersions were found to be dependent on composition and degree of postneutralization. But the chain extension and degree of preneutralization were observed to have little effect on the rheological behavior of the dispersions at a constant polyurethane (PU) concentration. The complex viscosity of the polyurethane dispersions increased dramatically at a critical concentration of polyurethane ($\phi = 0.43$), below which the viscosity increased slightly with composition. At this critical concentration the particles are crowded, and the observed viscosity increase is ascribed to the hydrodynamic interaction between the different particles. Furthermore, both G'' and G'' are strongly increased with increasing PU wt % in the dispersions (i.e., the higher the concentration of PU, the higher the values of G' and G''). At 46 wt % PU the values of G' and G'' are no longer frequency dependent, and G' is almost 1 order of magnitude higher than G'', indicating formation of a fractal-type gel. The viscoelastic material functions were well described by simple power law equations and a Maxwellian (Hookean) model with 2−3 relaxation modes based on PU concentration and degrees of postneutralization at 30 °C. Time−temperature superposition of the dynamic moduli was good at temperatures and PU concentrations below that of the critical gel, and the temperature dependence of the shift factors conformed well to predictions from an Arrhenius-type relation, enabling calculation of the flow activation energy of 45 kJ mol^{-1} for the PUDs. As expected, time−temperature superposition failed to represent the behavior of the PUDs near the critical gel point. While the results of this study indicate a number of similarities to critical gelling systems, observed deviations from the viscoelastic behavior of Brownian suspensions of hard spheres were obtained, indicating that a more complicated theory that explicitly takes the intrinsic interactions, concentrations, and size distributions of the PU particles into account may be necessary for a more accurate quantitative description of these special model PUDs with enhanced benefits.

Introduction

Polyurethane dispersions belong to a special class of colloidal dispersions that are mixtures of different chemical species where the interfacial area plays a dominant or at least an important role, so that their properties depend strongly on the interfacial forces or physicochemical interactions.[1,2] This important class of materials is very useful in many applications such as coatings, biological fluids, drilling muds, food, cosmetics, and pharmaceuticals. In general, a colloidal dispersion is stable when the droplets (discontinuous phase) persist uniformly in the liquid medium (continuous phase). The dispersion becomes unstable when the droplets diffuse together to form a single bigger droplet that leads to a reduction in the total surface area (coalescence) or to form an aggregate of particles without producing a new particle (flocculation). The role of polymer in stabilization or flocculation of colloidal dispersion has been studied extensively in the literature.[1−5]

In recent years, significant emphasis has been placed on the use of waterborne coating systems such as polyurethane dispersions (PUD) due to their health and environmental safety.[6−12] Design and control of these systems has been traditionally undertaken by trial and error methods due to their inherent complexity. These environmentally friendly products are used to reduce the VOC (volatile organic compounds) released into the atmosphere by solventborne systems and are expected to exhibit the same performance as that of conventional solventborne systems. Polyurethane dispersions can be tailored to various applications by varying the preparation method and chemical structures of the polyurethane. Typically a waterborne PUD is formed by preparing an isocyanate-terminated prepolymer, and a modifying polyol is used to incorporate carboxylic functionality in the prepolymer backbone. The prepolymer is then dispersed in water using a tertiary amine to produce ionic centers, thus stabilizing the polymer particle. The resulting chemical species is then chain-extended using a polyamine as described later.[12] Polyurethane dispersions are typically used in many application areas such as textile coatings, leather finishing, adhesives, sealants, plastic coatings, wood finishes, and glass fiber sizing, to an extent that depends on the preparation methods.[13−21] Because of their versatility and environmental friendliness, aqueous PUDs are now one of the most rapidly developing and active branches of PU chemistry and technology.

† Permanent address: Faculty of Science, Department of Chemistry, Cairo University, Orman-Giza 12613, Egypt. E-mail: Samy.Madbouly@usm.edu.

* To whom all correspondence should be addressed: Tel 601-266-5596; e-mail Joshua.Otaigbe@usm.edu.

10.1021/ma050453u CCC: $30.25
Published on Web 03/31/2005

Heretofore, much of the patents and journal articles on PUDs in the literature appear to focus almost exclusively on the application of these interesting systems. There are relatively little reported systematic studies on PUDs to generate basic data aimed at providing fundamental insights into the relationships among the polymer structure, rheological properties, and coating performance under conditions that the PUDs are likely to encounter during use. By systematically varying the solid content and particle size of the present PUDs, our long-range research program will shed light on how controlled changes in the strength and range of particle interactions alter the phase behavior, morphology, rheology, and mechanical properties. The intrinsic differences between the special PUDs of this study and conventional polymer colloids,[1,2] suspensions,[22−24] and emulsions[1,23] require that analyses of the PUDs be based on their actual behavior so as to generate accurate and useful data that will guide the synthesis, processing, and modeling of this important class of materials. It is hoped that the present study will provide a quantitative and qualitative experimental basis for any future theory development of the relatively new waterborne PUDs and the prediction of their rheological properties, increasing our level of understanding of the behavior of these systems. Another objective of our research is to stimulate further experimental work and a more scientific analysis of these useful industrial systems, leading to a reduction in high design and raw materials costs that is common to the trial and error methods currently used in industry.

A transition of liquid to solid structure as a result of gelation with increasing concentration has been reported for hard-sphere dispersions.[25−28] This transition is manifested as a nondecaying component of the dynamic structure factor and implies a structural arrest of the crowded suspension.[26−28] A similar phenomenon has been recently reported for weakly attractive soft colloids.[29,47] The gelation process in the soft colloids just mentioned was found to be intrinsically related to the fluid to solid transition, which is manifested as a kinetic arrest and is driven by the crowding or clusters of particles. This behavior is a characteristic of a wide range of soft materials that lose their ability to flow at high volume fractions.[29] Consequently, it is important to understand and control this transition process and in more general terms the different kinds of interactions between the particles during the liquid−solid transition in colloidal dispersions.

Many dispersions, including latex systems, are known to exhibit complex rheological behavior. Rheological properties of waterborne coating systems are of both practical importance and theoretical interest. In addition, the stability, digestibility, film-forming properties, and viscoelastic properties of PUDs are expected to be strongly dependent on their colloidal state, structure, and composition. It is therefore essential to understand the rheological behavior of these important dispersions so that they can be prepared and used in a controlled and reproducible manner. In this article we explore details of the rheological properties of a well-characterized model PUD system as functions of solid content, degree of pre- and postneutralization, chain extension, and temperature. The rheological data obtained will be interpreted using different theoretical principles such as the Cross model, Krieger−Dougherty equation, and time−temperature superposition (WLF). Where appropriate, the viscoelastic behavior of the PUDs will be compared to that of critical gelling systems and Brownian suspensions reported in the literature. It is expected that the rheological behavior of the PUDs can be controlled by changing the experimental parameters used here, providing a fundamental basis for optimizing their applications and performance in response-driven polymer film formation.

Experimental Section

Materials. Polyester polyol (Desmophen 1019-55), and isophorone diisocyanate (Desmodur-I) were supplied by Bayer MaterialScience, Pittsburgh, PA. Dimethylolpropionic acid (DMPA), dibutyltin dilaurate (DBTDL), 1-methylpyrrolidinone (NMP), triethylamine (TEA), hexamethylenediamine (HMDA), diethylamine (DEA), and tetrahydrofuran (THF) were received from Aldrich Chemical Co. Ethoxylated nonylphenol ammonium sulfate (Abex EP-110, Rhodia Chemicals, Cranbury, NJ) was used as a surfactant. Defoamer (Foamstar-111) was received from Cognis Co., Cincinnati, OH. All the materials were used as received.

Prepolymer Synthesis. A 250 mL round-bottom, four-necked flask with a mechanical stirrer, thermometer, condenser with nitrogen in/outlet, and a pipet outlet was used as a reactor. The polymerization was carried out in a constant temperature oil bath. Desmophen 1019-55 and DMPA were charged into the dried flask at 70 °C. While stirring, NMP (10 wt % based on total feed) was added, and stirring was continued until a homogenized mixture was obtained. Desmodur-I and DBTL were added, and stirring was continued for 30 min at this temperature. The mixture was heated to 80 °C for about 3 h to afford an NCO-terminated prepolymer. The NCO content during the reaction was determined using a standard dibutylamine back-titration method. Upon obtaining a theoretical NCO value, the prepolymers were cooled to 60 °C, and the neutralizing solution, i.e., TEA (DMPA equiv) dissolved in NMP (2 wt %) was added and stirred for 30 min while maintaining the temperature at 60 °C.

Dispersion and Chain Extension. Dispersion of PU was accomplished by adding the prepolymer to the mixture of water and surfactant (4 wt % based on total solid). Agitation was maintained at 750 rpm. After 20 min, 20 wt % solution of HMDA in water was added over a period of 30 min, and chain extension was carried out for the next 1 h. Subsequently, defoamer (Foamstar-I) was added, and stirring was continued for 5 min at a speed of 250 rpm. The solids content of the dispersion was changed from 24 to 46 wt % PU. For experiments requiring control of the polymer molecular weight, diethylamine was included in the chain extension step. In the preparation of all polymers the ratio of isocyanate groups/amine groups (from chain extension/termination) was 1.1/1.

Particle Size Measurement. Particle sizes (diameter in nanometers) were determined using a Microtrac UPA 250 light scattering ultrafine particle analyzer.[31] The sample was diluted to the required concentration with distilled water before measurement.

Rheological Measurements. The viscoelastic measurements were done using an Advanced Rheometerics Expansion System (ARES, Rheometrics Inc.) equipped with two 25 and 40 mm parallel plates diameter. For very low-viscosity samples, we used a Physica MCR 501 rheometer with Couette and 25 mm diameter cup. To prevent dehydration of the PUD, a thin layer of low-viscosity silicone oil was applied to the air/sample interface. In this study, the following rheological experiments were performed:

1. Strain sweep at a constant temperature and frequency range of 0.1−100 rad/s to obtain the linear viscoelastic range of the dispersions.

2. A time sweep at a constant temperature and frequency to obtain steady state and thus ensure that the measurements were carried out under equilibrium condition.

3. Frequency sweep at a given temperature (30−90 °C) in the linear viscoelastic region (strain amplitude ≤10% strain)

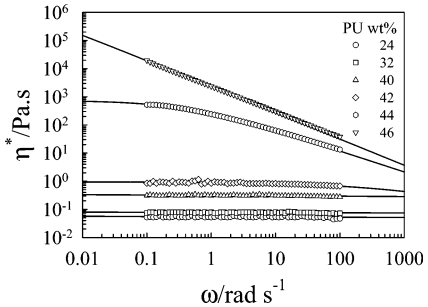

Figure 1. Variation of η^* as a function of shear frequency for different PU content at 30 °C. The lines are computed from eq 1 using the nonlinear regression technique.

Scheme 1. Elementary Steps for the Synthesis of PUD

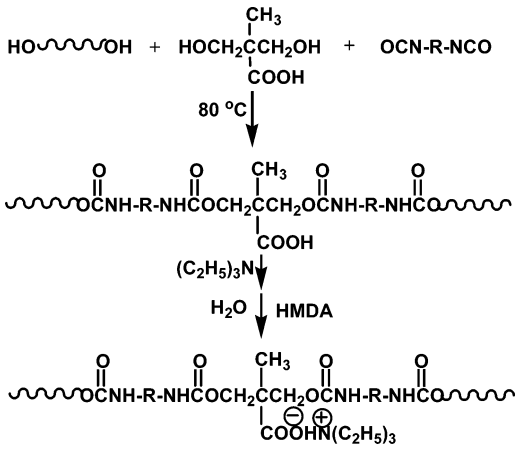

to obtain the dynamic shear moduli, i.e., storage shear modulus, G', and loss modulus, G''. The master curves were obtained by horizontal shifts of the experimental data. The zero-shear viscosities (η_0) of the blends were calculated by fitting the $|\eta^*|$ vs ω data to the Cross model.[30]

Results and Discussion

The synthesis of PUD is presented in Scheme 1. The role of the ionic groups is to provide a stable PU dispersion in water.

Additional details of the synthesis and chemistry of the process are given elsewhere.[31]

Effect of Solid Content. The double-logarithmic scale of the complex viscosities of PUD as a function of shear frequency at 30 °C for different PU concentrations is shown in Figure 1. Clearly, this figure shows that the viscosities of the dispersions are strongly influenced by the solid concentration of PU. Frequency-independent complex viscosity behavior is observed for all the dispersions having solid concentrations of PU ≤ 42 wt %. The viscosity increased dramatically (about 4 orders of magnitude) when the concentration of PU was increased from 24 to 46 wt %. In addition, the viscosity decreased with increasing shear frequency. The frequency (ω) dependence of $|\eta^*|$ is independent of ω if ω is sufficiently smaller than the reciprocal of the characteristic times λ of all modes, and the decrease of $|\eta^*|$ with ω simply indicates that some modes have $1/\lambda$ smaller than ω as will be shown later.

The frequency dependence of the dynamic viscosity of PUD can be expressed through the Cross model[30] by the following equation:

$$\eta = \frac{\eta_0}{1 + (\omega/\omega_c)^{\beta}} \tag{1}$$

where η_0 is the zero-shear viscosity, ω_c is the critical shear frequency value at which the viscosity decreases to half its initial value, and β is a material constant that depends on the nature of the dispersion. Equation 1 was used to calculate η_0 as a fitting parameter to the experimental results using nonlinear regression analysis. An excellent description of the data was obtained as shown in Figure 1. Table 1 represents the fitting parameters that were obtained from the regression. Here the lines in Figure 1 are computed from eq 1 using the parameters listed in Table 1, while the points are experimental data.

Figure 2 illustrates the volume fraction (ϕ) dependence of the dimensionless viscosity of the dispersions, η_r (reduced by the solvent viscosity). The critical volume fraction (ϕ_c) at which the viscosity of the dispersions increased strongly was determined using the Krieger–Dougherty equation:[32]

$$\eta_r = \left(1 - \frac{\phi}{\phi_c}\right)^{-k\phi_c} \tag{2}$$

with

$$\eta_r = \frac{\eta_D}{\eta_S} \tag{3}$$

where k is a shape parameter, η_D is the viscosity of dispersions, and η_S is the viscosity of solvent. The experimental data can be described using the above equation, where the symbols are experimental data while the line is the calculated line using k and ϕ_c as fitting parameters. It must be stated here that the data shown in Figure 2 are the values of the zero-shear viscosity of the dispersions (i.e., $\eta_D = \eta_0$ only for this figure). The value of ϕ_c obtained from this regression analysis was found to be 0.43. The Krieger–Dougherty equation works well for hard-sphere dispersions with volume fraction less than 0.55. It is well-known that the value of ϕ_c strongly depends on the system under consideration. For example, small, monodispersed samples show lower value of ϕ_c than large ones and ϕ_c increases with polydispersity.[33] This rheological behavior depicted in Figure 2 is governed by the interplay between the particle–particle interaction (repulsive force between the similar charges surrounding the particles) and hydrodynamic interaction. The interaction potential depends on the charge density on the particle surface. It is essential to mention here that all the samples of different volume fractions were prepared at constant concentration of internal surfactant (5.5 wt % DMPA);[31] i.e., all the particles have similar charge density regardless of the change in the volume fraction. Therefore, the repulsive force between particles should be constant for all concentration. Another important factor that should be considered is the large increase of the particle size with concentration as clearly depicted in the inset plot of Figure 2. The increase in viscosity with concentration is directly related to the increase in particle size. At low concentration the effect of particle size is insignificant because the particles are far apart and do not significantly interact with each other. On the other hand, at high concentration the particles become very crowded, and the viscosity increases due

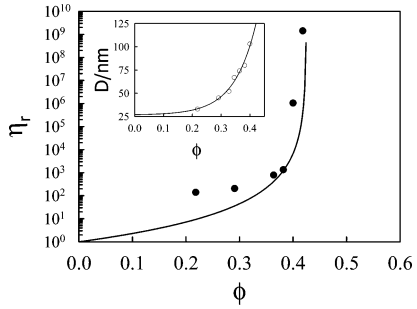

Figure 2. Volume fraction dependence of reduced viscosity, η_r, at 30 °C. The line passing through the experimental data is the fitting line of eq 2 using the nonlinear regression technique. The inset plot shows the particle diameter as a function of volume fraction.

Table 1. Characteristic Rheological Parameters for the PUD of Different Concentrations Using Eq 1

PU/wt %	η_0/Pa·s	ω_c/rad s^{-1}	β
46	9.9×10^5	0.01	0.87
44	738	0.4	0.74
42	0.94	677	0.44
40	0.316	836	0.8
32	0.14	4.6×10^5	0.31
24	0.098	5.8×10^5	0.287

to the significant increase in the hydrodynamic interactions between the particles. On the basis of the above discussion, it appears that the interaction potential due to the repulsive force between the similar charge particles is significant at low concentration. However, on the other hand, at high concentration, the particle size increases, and both the interparticle distance and interaction potential decrease, making the hydrodynamic interaction the only factor responsible for the observed increase in the viscosity of PUDs. The poor fitting of the experimental data with eq 2 is mainly due to two reasons: the first one is that eq 2 is normally used for hard-sphere suspensions containing particles that are not deformable under shear flow, and the second reason is ascribed to the observed increase in the particle size of the PU dispersion with increasing volume fraction (see the inset plot of Figure 2).

A simple model for rheological behavior of concentrated colloidal dispersions of hard spheres has been developed by Brady.[34] This model specifies that the viscosity diverges at random close packing because the number of contacting particles becomes infinite, and the short-time self-diffusivity vanishes as the touching particles are stuck by the hydrodynamic lubrication forces.[34] In addition, optical measurement of the contributions of colloidal forces to rheology of concentrated suspensions has been reported by Bender et al.[35] The normalized stress−optical coefficients calculated from dichroism and viscosity measurements of near hard-sphere colloidal suspensions were found to be relatively constant with respect to the volume.[35]

The master curve of the dynamic viscosity of PUD at different concentrations can be obtained by normalizing the relative viscosity (η_r) by zero-shear viscosity and the shear frequency by the critical shear frequency (ω_c) for each concentration.[36] This can be simply described by the following relation:

$$\eta_r/\eta_0 = f(\omega/\omega_c)^\beta \tag{4}$$

where $f(\omega/\omega_c)^\beta$ is assumed to be a universal function, independent of molecular weight, concentration, and

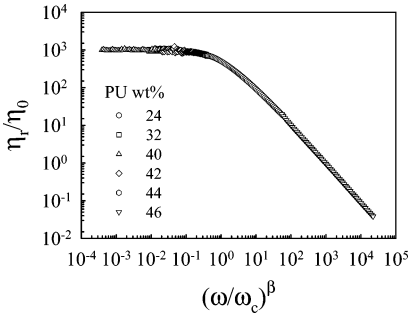

Figure 3. Master curve of normalized viscosity, η_r/η_0, at 30 °C for different PU concentrations.

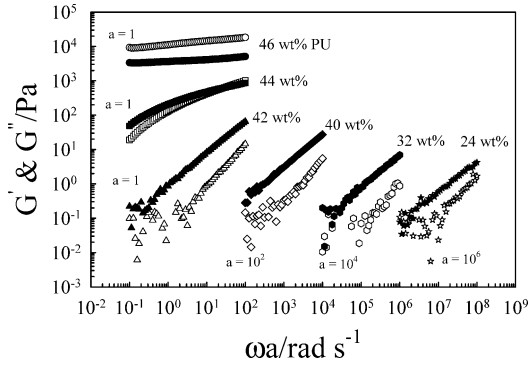

Figure 4. Dynamic shear moduli, G' (open symbols) and G'' (solid symbols), as a function of shear frequency for different PU contents at 30 °C. The x-axis is extended by a factor a = 1−10000 to obtain a valid comparison.

temperature. From eq 4 it is apparent that the parameters η_0, ω_c, and β are crucial for calculating the master curve. These parameters were accurately evaluated for different concentrations of PU at 30 °C (Table 1) by fitting the classical frequency dependence of dynamic viscosity to eq 1, as shown in Figure 1. A satisfactory master curve for PUD was obtained at 30 °C as shown in Figure 3. The master curve shows frequency-independent behavior at small shear frequency range followed by strong frequency-dependent behavior at high frequencies. This is an important result that should be useful in predicting the behavior of the PUDs, especially under deformation and flow conditions that are experimentally inaccessible.

Figure 4 demonstrates the effect of PU concentration on the dynamic shear moduli, G' and G'', at 30 °C. The x-axis was shifted to higher frequency range by a factor, a, ranging from 1 to 10^6 as shown in the figure to obtain a valid comparison. One can see that the values of both G' and G'' are increased with increasing PU wt % in the dispersions (i.e., the higher the concentration of PU, the higher the values of G' and G''). The fact that the magnitudes of G' and G'' are increased strongly with composition (especially at 44 and 46 wt % PU) suggests that PUD can form a critical gel (fractal structure) with high PU content. It is apparent that the magnitudes of G' are much lower than that of G'' for all concentrations in the range of PU wt % ≤ 42, and both of them are shear frequency dependent. For 44% PU the values of G' becomes a little higher than G'' only at the higher frequency range, indicating that 44% PU is located in the gel boundary. At 46 wt % PU the values of G' and G'' are no longer frequency dependent, and G' is almost 1 order of magnitude higher than G''. This is a typical behavior for the formation of a fractal structure or gel that is attributed to the strong interaction between the

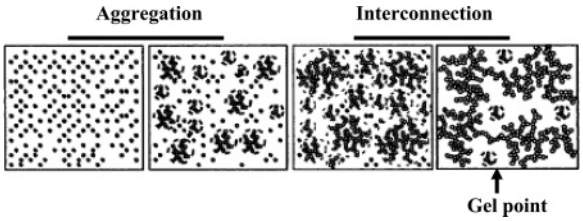

Figure 5. Schematic diagram of aggregation and gel formation (adapted from ref 37).

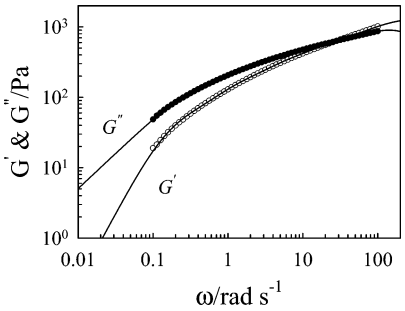

Figure 6. Dynamic shear moduli G' and G'' as a function of shear frequency for 44 wt % PU at 30 °C. The solid lines are calculated from Maxwell model of multiple modes (eqs 5 and 6).

particles, leading to optimal packing. The experimental fact that the magnitudes of G' and G'' are frequency independent is ascribed to the formation of an equilibrium modulus, G_{eq}, a typical criterion for the formation of an elastic gel. It is remarkable that the gelation behavior of PUD with 46 wt % PU is in good agreement with the kinetic modeling of aggregation and gel formation in quiescent dispersions of polymer colloids postulated by Lattuada et al.[37] On the basis of this model, the gel is formed by fractal aggregation that have grown to such an extent that they occupy the total volume of the dispersion. To form the network, the aggregates have to interconnect with each other. This interconnection step is quite different from the preceding aggregation step in that the aggregates do not diffuse randomly but directly experience their nearest neighbors. Therefore, they have to move cooperatively in order to rearrange their spatial configuration substantially, becoming increasingly unlikely near the gel point.[37] Figure 5 shows schematically that the formation of gel, the aggregation, and interconnection steps are not identical as already discussed.[37] On the basis of the preceding discussion, it is apparent that the viscoelastic behavior of the PUDs explored in this paper can be divided into two different regimes. At wt % PU ≥ 44 (regime 1), the dispersions behave as critically gelling systems;[38,39] however, in the second regime at wt % PU ≤ 42, the dispersions behave as typical Brownian suspensions.[34,35,40]

The above dynamic moduli data can be modeled by the generalized Maxwell model/Maxwell−Wiechert model according to the following equations:[24]

$$G'(\omega) = \sum_0^\infty \frac{G_i \omega_i^2 \lambda_i^2}{1 + \omega_i^2 \lambda_i^2} \tag{5}$$

$$G''(\omega) = \sum_0^\infty \frac{G_i \omega_i \lambda_i}{1 + \omega_i^2 \lambda_i^2} \tag{6}$$

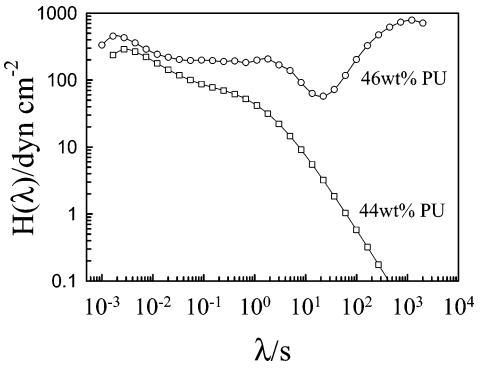

Figure 7. Relaxation spectra of 44 and 46 wt % PUDs at 30 °C.

where λ_i is the characteristic relaxation time, G_i is the elastic constant, ω is the angular frequency, and i indicates the number of modes required to fit the dynamic moduli. The experimental data shown in Figure 4 can be fitted well with a number of Maxwell elements connected in series as described by the above equations. Figure 6 shows an example of the dynamic shear moduli for 44 wt % PU as a function of angular frequency. The lines dawn through the experimental data are the fitting lines using the Maxwell model. An excellent description of the data was obtained with five Maxwell elements in series.

The distribution of relaxation times for PUDs can be examined on the basis of the inverse Laplace transformation:

$$G'(\omega) = \int_{-\infty}^{\infty} H(\lambda) \left[\frac{\omega^2 \lambda^2}{1 + \omega^2 \lambda^2} \right] \mathrm{d}(\ln \lambda) \tag{7}$$

$$G''(\omega) = \int_{-\infty}^{\infty} H(\lambda) \left[\frac{\omega \lambda}{1 + \omega^2 \lambda^2} \right] \mathrm{d}(\ln \lambda) \tag{8}$$

where $H(\lambda)$ is the relaxation spectrum and λ is the relaxation time. Figure 7 shows the relaxation spectra for 46 and 44 wt % PU samples. Three relaxation peaks can be clearly seen for the 46 wt % PU; however, only two relaxation peaks were observed for the 44 wt % PU sample. The relaxation peak appearing at very long relaxation time for the sample of 46 wt % PU is related to the dynamics of the highly solid structure of the fractal gel (G' is much higher than G'' as shown in Figure 4) that is typically characterized by a very long relaxation time. This relaxation peak does not appear in any other composition of lower PU concentration. Another two relaxation peaks appear around 0.002 and 2 s for the two samples showing a slight composition effect. Clearly, these results show that the variation of volume fraction of PU leads to a significant change in the relaxation spectrum particularly near the critical composition where the dispersion changes from a liquidlike consistency to a solidlike structure (fractal gel).

2. Effect of Degree of Neutralization of the PUD. The degree of preneutralization was found to have no significant effect on the rheological behavior of PUD. The PUD (32 wt % PU) has a nearly constant viscosity, i.e., frequency-independent behavior regardless of the degree of preneutralization, as shown in Figure 8. However, the viscosity of PUD was changed dramatically by the degree of postneutralization. Figure 9 shows the shear frequency dependence of the complex viscosity of PUD with different degrees of postneutralization at

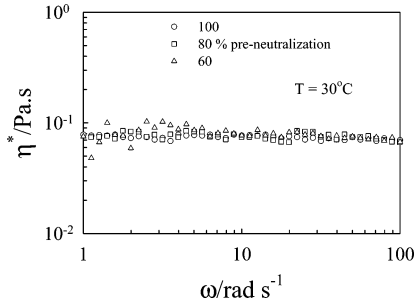

Figure 8. Shear frequency dependence of dynamic viscosity for PUD of different degrees of preneutralization at 30 °C.

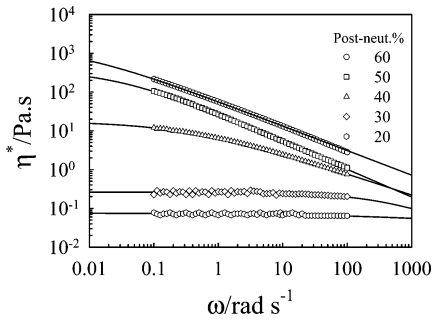

Figure 9. Variation of $|\eta^*|$ as a function of shear frequency for PUD of different degrees of postneutralization at 30 °C. The lines are computed from eq 1 using the nonlinear regression technique.

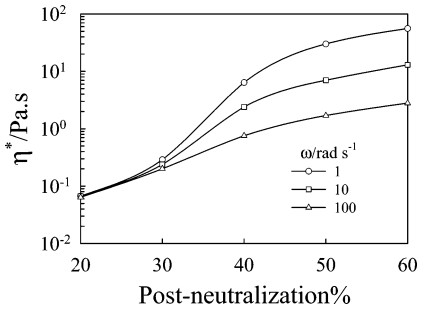

Figure 10. Effect of degree of postneutralization on the dynamic viscosity of PUD at 30 °C for different shear frequencies.

Table 2. Characteristic Rheological Parameters for the PUD of Different Degree of Post-Neutralization Using Eq 1

postneutralization/%	η_0/Pa·s	ω_c/rad s^{-1}	β
60	1.6×10^3	0.0053	0.63
50	3.6×10^2	0.026	0.71
40	15.6	0.37	0.55
30	0.26	350	0.68
20	0.076	3.6×10^3	0.27

30 °C. The viscosity increases dramatically (3 orders of magnitude) by increasing the degree of postneutralization from 30 to 60%. The solid lines are computed from the eq 1. The fitting parameters obtained from this regression are listed in Table 2. Figure 10 shows how the viscosity at different shear frequencies increases greatly with increasing degree of postneutralization. The value of $|\eta^*|$ is almost constant at different frequencies for the sample of 20% postneutralization (frequency-independent behavior) while it is strongly dependent on frequency for higher degrees of postneutralization particularly for 40−60%. This dramatic increase in the viscosity of PUD is attributed to the trapping of the −COOH groups inside the core of the particle. During

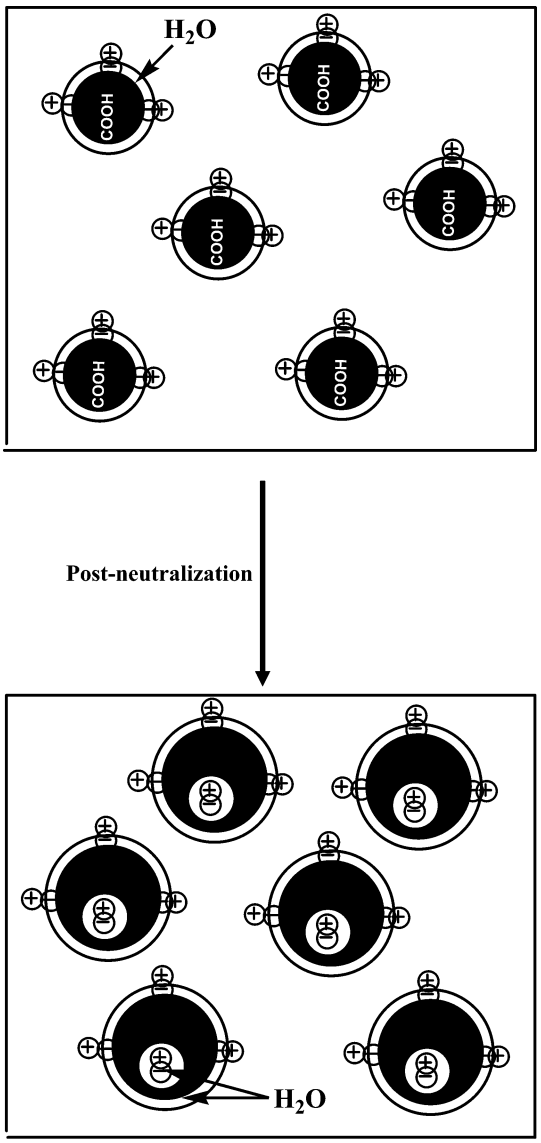

Figure 11. Schematic diagram showing the effect of postneutralization on the particle size.

the postneutralization process the −COOH groups will be converted to the hydrophilic $-COO^-HN^+(C_2H_5)_3$ groups that can attract some water molecules inside the particle, leading to an increase in the particle size while keeping the number of the particles constant. Consequently, the free volume decreases and the viscosity increases. The mechanism of the PUD neutralization reactions is described in the Experimental Section. The decrease in the free volume and the increase in the particle size are illustrated in Figure 11. Additional details on the chemical reaction mechanisms of the PUD neutralizations are given elsewhere.[31]

It is instructive to construct a master curve for the reduced viscosity (η_r) of PUD with different degrees of postneutralization as defined by eq 4. Similar behavior to the effect of solid content (Figure 3) was obtained as shown in Figure 12. On the basis of this experimental finding, it is apparent that the effect of increasing the degree of postneutralization on the PUD rheology is analogous to that of increasing solid concentration as already discussed.

The dynamic shear moduli, G' and G'' for the PUD of different degrees of postneutralization at 30 °C are shown in Figure 13. Again, similar to the composition

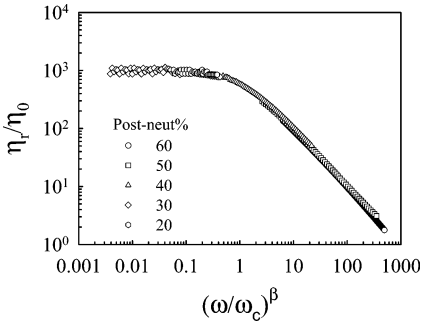

Figure 12. Master curve of normalized viscosity, η_r/η_0, at 30 °C for different PUD of different degrees of postneutralization.

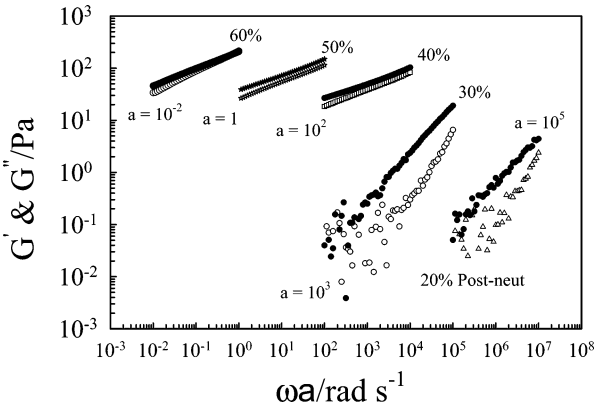

Figure 13. Dynamic shear moduli, G' (open symbols) and G'' (solid symbols), as a function of shear frequency for different degrees of postneutralization at 30 °C.

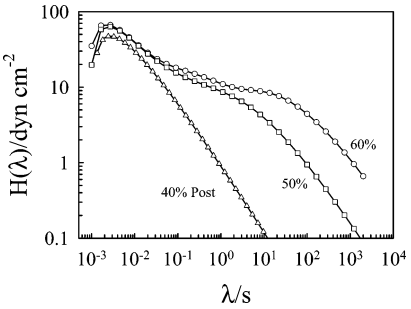

Figure 14. Effect of degree of postneutralization on the relaxation spectra of PUDs.

effect, the G' and G'' increase dramatically with increasing degree of postneutralization due to the increase in the particle size and the decrease in the free volume as already discussed. The value of G' is lower than the value of G'' over the whole frequency range for 20−50% postneutralization. However, G' is found to be equal to G'' at the high frequency range only for the case of 60% postneutralization. This behavior indicates that the PUD of 60% postneutralization is very close to the gel boundary and also reflects the high probability of the big particles to interact with each other relative to the small ones.

The effect of degree of postneutralization on the distribution of relaxation times is shown in Figure 14. Obviously, the relaxation spectrum changes significantly with the variation of the degree of postneutralization. At high degree of postneutralization such as 60 and 50%, two relaxation processes are detected; however, only one relaxation process is observed at low degrees of postneutralization, such as 40% (Figure 14). The relaxation peak appearing at low relaxation time

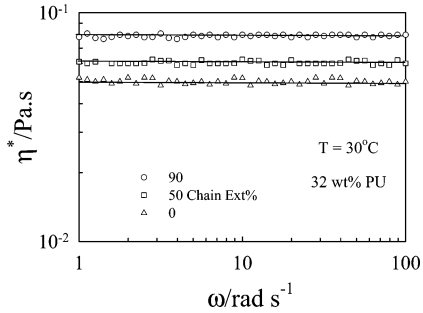

Figure 15. Frequency dependence of dynamic viscosity for PUD of different degrees of chain extension at 30 °C.

(0.0025 s) does not change with the different degree of postneutralization. But the peak appearing at long relaxation time is shifted to longer relaxation time with increasing degree of postneutralization and disappearing with decreasing degree of postneutralization as shown for 40 wt % postneutralization (Figure 14). Therefore, this relaxation peak is directly related to the long relaxation mode of the high viscosity of the PU dispersion. With decreasing degree of postneutralization, the viscosity decreases strongly and consequently the long relaxation peak disappears.

Effect of Temperature and Chain Extension. The degree of chain extension was found to have a negligible influence on both particle size and viscosity of the PUD. Figure 15 shows the frequency dependence of $|\eta^*|$ for PUD of different degrees of chain extension. The viscosity of PUD shows frequency-independent behavior and increases slightly with increasing degree of chain extension. Although the molecular weight of PU increases by about 4 times with increasing chain extension from 0 to 90%, the viscosity of the dispersions does not change significantly. This observation is attributed to the fact that all the dispersions have almost the same particle size and particle size distribution regardless of the differences in the chain extension. This similarity in both particle size and its distribution leads to similar interaction between the particles in each dispersion and consequently similar viscosity. The experimental procedure used for chain extension is responsible for the observed little change in the viscosity of PUDs. As described in the Experimental Section, we prepared the dispersions prior to chain extension, making it possible to maintain the particle sizes and their distribution and consequently insignificant change in the viscosity of PUDs. This confirms our expectation that rheology is a sensitive and reliable probe for design and control of PUDs.

To investigate the effect of temperature on the rheological behavior of the PUD, we used one highly viscous example (i.e., 60% postneutralization) for this part of this study. The double-logarithmic scale of the complex viscosities of this sample at different temperatures is represented in Figure 16. The frequency dependence of the viscosity of this PUD composition can be expressed by eq 1, as shown by the fitting lines through the experimental points. Excellent descriptions of the data are obtained using this model. The increase in temperature from 70 to 90 °C led to a dramatic increase in the viscosity as Figure 16 shows. This increase in the viscosity is consistent with the sample behaving as solidlike structure. This behavior is not observed for all the PUD samples; for example, the sample of 0% postneutralization (i.e., 100% preneutralization) does not show any increase in viscosity with increasing

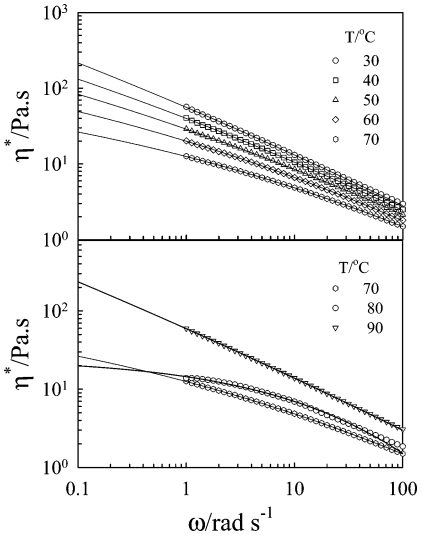

Figure 16. Frequency dependence of dynamic viscosity for PUD of 60% postneutralization at different temperatures. Solid lines are fits of eq 1 to the experimental data.

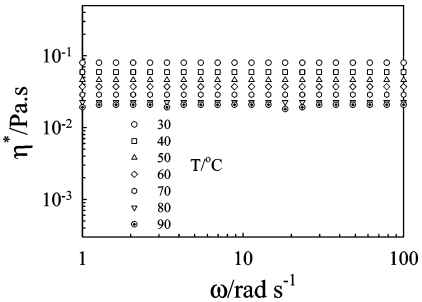

Figure 17. Frequency dependence of dynamic viscosity for PUD of 0% postneutralization (i.e., 100% preneutralization) at different temperatures.

temperature (see Figure 17). These experimental results point to the fact that the increase in the viscosity is related to a typical gelation process induced thermally. This process is thought to be a function only of the particle size; the bigger the particle, the higher the possibility for gel formation. In the case of 60% postneutralization the particle size is 300 nm, but it is only 45 nm for the 0% postneutralization.[31] Therefore, the thermal energy increases the interaction between the big particles, leading to gel formation. This energy is not sufficient to induce gelation in the case of small particle size (i.e., 0% postneutralization). On the basis of this experimental result, it is clear that the increase in viscosity with increasing temperature is not related to the evaporation of water. In addition, we confirmed the formation of gel by heating the dispersions in tightly closed glass bottles at around 70 °C in a water bath for 2 h. The sample of 60% postneutralization changed to a solid gel, but the sample of 0% postneutralization does not show any obvious increase in the viscosity, and it remained in the liquid state throughout the heating period. Details of gelation process and its kinetics of PUD as functions of temperature, time, and concentration will be considered separately in another publication.

It is reasonable to expect that the time−temperature superposition principle, WLF, might be affected by the formation of gel at high temperature. To check the validity of the WLF superposition principle, we measured the frequency dependence of the dynamic shear moduli, G' and G'', over a wide range of temperature

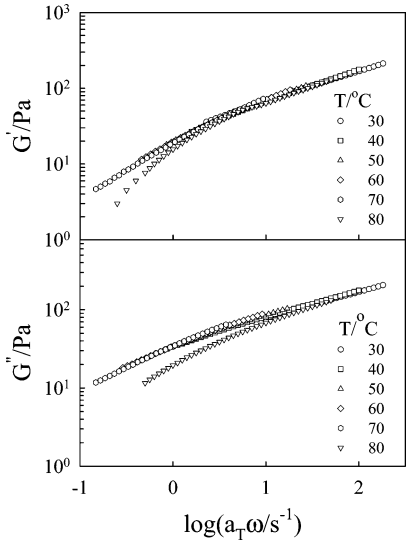

Figure 18. Master curves of storage and loss moduli at a reference temperature of 40 °C for PUD of 60% postneutralization.

exceeding the gel temperature i.e., up to 80 °C. The master curves of the dynamic shear moduli, G' and G'', can be constructed on the basis of thermorheological simplicity; for example, the storage modulus can be superimposed by horizontal shifts along the x-axis (frequency axis) according to the following equation

$$G'(\omega a_T, T_0) = G'(\omega, T) \tag{9}$$

where a_T is the horizontal shift factor and T_0 is the reference temperature. The time−temperature superposition increases the accessible frequency window of the linear viscoelastic experiments. This principle applies to stable materials without any physical or chemical reaction during the dynamic measurements, and only the effect of temperature on the relaxation process is considered. Therefore, the principle works well when the stress-sustaining structure in the system does not change with temperature and relaxation times of all modes of this structure change with temperature by the same factor. Figure 18 shows the master curves of the dynamic shear moduli, G' and G'', for 60% postneutralization PUD at T_0 = 40 °C. It is apparent from this figure that the WLF principle is only valid for temperatures lower than 80 °C; the WLF principle failed for $T \geq 80$ °C. This can be seen very clearly in the low-frequency region as a deviation from the terminal slopes in both G' and G'' curves. This deviation is attributed to the gelation process of the sample at high temperature (i.e., formation of solidlike structure with very long relaxation time). Near the gel point a lack of superimposability of the viscoelastic response at low frequencies characterized is attributed to the contribution of longest relaxation mode to the viscoelastic material function at the onset of gel formation. This gelation process of the sample during the dynamic measurement strongly influences the level of sustainable stress (i.e., G'). The breakdown of WLF principle has been observed for other polymeric materials such as block copolymers near the order−disorder transition[41] and polymer blends at the liquid−liquid transition.[42,43]

This deviation from the WLF principle can also be clearly seen in the modified Cole−Cole analyses (G'' vs G') depicted in Figure 19 (the curves start to deviate at

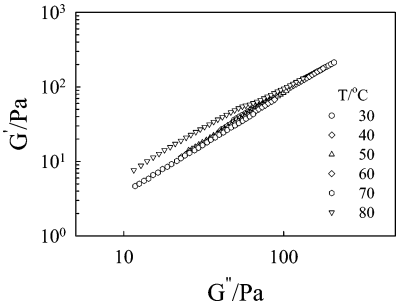

Figure 19. Cole−Cole plot for PUD of 60% postneutralization at different temperatures.

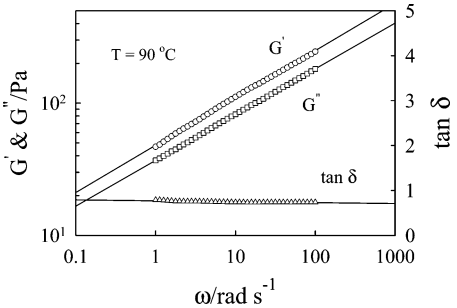

Figure 20. Frequency dependence of G', G'', and tan δ at 90 °C. The lines passing through G' and G'' data points show the power law behavior.

80 °C). At 90 °C, G' exceeds G'', illustrating a typical behavior for an elastic gel (see Figure 20). Both G' and G'' show the following power law behavior over the entire range of frequency:

$$G' \sim G'' \sim \omega^n \tag{10}$$

Based on the Kramers−Kronig relationship, the loss tangent at the gel point is given by[44]

$$\tan \delta = \frac{G''(\omega)}{G'(\omega)} = \tan \frac{2\pi}{2} = \text{constant} \tag{11}$$

The critical behavior emerges when the stress-generating gel has a self-similarly bifurcated structure (fractal structure) over a wide range of frequency.[44] The values of the exponent n obtained from the slopes of these two power laws are 0.35 and 0.34, respectively. This value is much lower than one, implying that the sample changes to an elastic or rigid gel at high temperature.[45] In addition, tan δ is constant and independent of the shear frequency as shown in Figure 20, confirming the formation of fractal gel based on the above equation.

The temperature dependence of the shift factor can be studied using the Arrhenius (eq 12) and the WLF (Williams−Landel−Ferry) (eq 13) expressions:[46]

$$\log a_T = \frac{E_A}{2.303R}\left(\frac{1}{T} - \frac{1}{T_0}\right) \tag{12}$$

$$\log a_T = \frac{-c_1(T - T_0)}{c_2 + (T - T_0)} \tag{13}$$

where R is the universal gas constant, E_A is the activation energy of flow, and c_1 and c_2 are the WLF parameters. Figure 21 shows the temperature dependence of the shift factor a_T for the data of Figure 18. The experimental points are fitted by the WLF equation using c_1 and c_2 as fitting parameters. The data are well

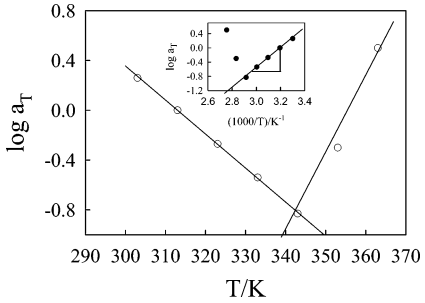

Figure 21. Shift factor a_T as a function of temperature for PUD of 60% postneutralization. The inset plot demonstrates the Arrhenius-type plot for the temperature dependence of a_T.

described by this equation at $T \leq 70$ °C. At higher temperatures the shift factor increases dramatically as seen in Figure 21. The inset plot of this figure shows the Arrhenius-type plot for the same experimental data; the value of the E_A obtained from the slope of the straight line in the temperature range $T \leq 70$ °C is 45 kJ/mol.

Conclusions

Rheological behavior of well-characterized model waterborne PUDs as functions of solid content, chain extension, pre-/postneutralization, and temperature has been extensively investigated for the first time to our knowledge. The complex viscosity of the PUD increases dramatically at a critical concentration of PU ($\phi = 0.43$), below which the viscosity increases slightly with composition. At this critical concentration the particles are very crowded, and the viscosity increases due to the hydrodynamic interaction between the different particles. The degree of preneutralization was found to have no effect on the rheological behavior of PUD. On the other hand, the viscoelastic properties changed dramatically by varying the degree of postneutralization. With increasing degree of postneutralization the steep viscosity increase is attributed to the increase in the particle size and the associated decrease in the free volume. The degree of chain extension was found to have a negligible effect on the rheological behavior of PUD. The viscoelastic material functions are well described by simple power-law equations, WLF principle, and a Maxwellian (Hookean) model with up to three relaxation times at certain PU concentrations and degrees of postneutralization at 30 °C. This study demonstrates that PUDs possess rich rheological behavior within experimentally accessible shear frequencies and can therefore serve as excellent model systems for exploring details of rheology and macromolecular structure dynamics of this class of industrially useful aqueous polymer dispersion with enhanced benefits in a number of new and existing applications. The experiments point to the need for a theory that explicitly takes the special interactions, concentrations, large surface area, size distribution, and the soft deformable nature of the PU particles into account.

Acknowledgment. We thank the Robert M. Hearin Support Foundation and Bayer MaterialScience, Pittsburgh, PA, for their support of this research. Partial support of this work from the National Science Foundation MRSEC (DMR 0213883) is gratefully acknowledged. We thank Anton Paar USA for providing us with direct access to their new MCR 501 rheometer. The helpful comments from the anonymous reviewer that

increased the quality of the manuscript are greatly appreciated.

References and Notes

(1) Goodwin, J. W. *Colloids and Interfaces with Surfactants and Polymers: An Introduction*; Wiley: New York, 2004.
(2) Russel, W. B.; Saville, D. A.; Schowalter, W. R. *Colloidal Dispersions;* Cambridge University Press: New York, 1989.
(3) de Gennes, P. G. *Adv. Colloid Interface Sci.* **1987**, *27*, 189.
(4) Ilett, S. M.; Orrock, A.; Poon, W. C. K.; Pusey, P. N. *Phys. Rev. E* **1995**, *51*, 1344.
(5) Napper, D. H. *Polymeric Stablization of Colloidal Dispersions*; Academic: New York, 1983.
(6) Markusch, P. H.; Tirpak, R. E. Symposium New Orleans, LA, 1990.
(7) Kim, B. Y.; Kim, T. K. *J. Appl. Polym. Sci.* **1991**, *43*, 393.
(8) Kim, C. K.; Kim, B. K. *J. Appl. Polym. Sci.* **1991**, *43*, 2295.
(9) Chan, W. C.; Chen, S. A. *Polymer* **1993**, *43*, 1265.
(10) Dreja, M.; Heine, B.; Tieke, B.; Junkers, G. *J. Colloid Interface Sci.* **1997**, *181*, 131−140.
(11) Wicks, Z. W.; Wicks, D. A.; Rosthauser, J. W. *Prog. Org. Coat.* **2002**, *44*, 161−183.
(12) Howarth, G. A. *Surf. Coat. Int., Part B: Coat. Trans*. **2003**, *86*, 111.
(13) Lorenz, O.; August, H. J.; Hick, H.; Triekes, F. *Angew. Makromol. Chem.* **1977**, *63*, 11.
(14) Lorenz, O.; Hick, H. *Angew. Makromol. Chem.* **1978**, *72*, 115.
(15) Markusch, P. H. U.S. Pat. 4,408,008, 1981.
(16) Hsu, S. L.; Xiao, H. X.; Szmant, H. H.; Frisch, K. C. *J. Appl. Polym. Sci.* **1984**, *29*, 2467.
(17) Kim, B. K.; Lee, Y. M. *Colloid Polym. Sci.* **1992**, *270*, 956.
(18) Kim, B. K.; Lee, J. C. *J. Polym. Sci., Polym. Chem.* **1996**, *34*, 1095.
(19) Wicks, D. A.; Wicks, Z. W. *Prog. Org. Coat.* **1999**, *36*, 148.
(20) Hourston, D. J.; Williams, G. D.; Satguru, R.; Padget, J. C.; Pears, D. *J. Appl. Polym. Sci.* **1999**, *74*, 556.
(21) Wicks, D. A.; Wicks, Z. W. *Prog. Org. Coat.* **2001**, *43*, 131.
(22) Metzner, A. B. *J. Rheol.* **1985**, *29*, 739.
(23) Barnes, H. A.; Hutton, J. F.; Walters, K. *An Introduction to Rheology*; Elsevier: Amsterdam, 1989.
(24) Macosko, C. W. *Rheological Principles, Measurements and Applications;* Wiley-VCH: New York, 1994.
(25) Russel, W. B. *Colloidal Dispersions*; Cambridge University Press: New York, 1989.
(26) van Megen, W.; Underwood, S. M. *Phys. Rev. E* **1994**, *49*, 4206.
(27) Pusey, P. N.; van Megen, W. *Phys. Rev. Lett.* **1987**, *59*, 2083.
(28) Stiakakis, E.; Vlassopoulos, D.; Loppinet, B.; Roovers, J.; Meier, G. *Phys. Rev. E* **2002**, *66*, 051804.
(29) Cates, M. E.; Evans, M. R. *Soft and Fragile Matter: Metastability and Flow;* IOP Publishing: Bristol, 2000.
(30) Cross, M. M. *J. Colloid Sci.* **1965**, *20*, 417.
(31) Nanda, A. K.; Wicks, D. A.; Madbouly, S. A.; Otaigbe, J. U. *J. Appl. Polym. Sci.*, submitted.
(32) Krieger, I. M.; Dougherty, T. J. *Trans. Soc. Rheol. III* **1959**, 137.
(33) Farris, R. J. *Trans. Soc. Rheol. III* **1968**, *2*, 281.
(34) Brady, J. F. *J. Chem. Phys.* **1993**, *99*, 567.
(35) Bender, J. W.; Wagner, N. J. *J. Colloid Interface Sci.* **1995**, *172*, 171.
(36) Jones, A. R.; Leary, B.; Boger, D. V. *J. Colloid Interface Sci.* **1992**, *150*, 84.
(37) Lattuada, M.; Sandkuhler, P.; Wu, H.; Sefcik, J.; Morbidelli, M. *Macromol. Symp.* **2004**, *206*, 307.
(38) Winter, H. H.; Chambon, F. *J. Rheol.* **1986**, *30*, 367.
(39) Chambon, F.; Winter, H. H. *J. Rheol.* **1987**, *31*, 683.
(40) Shikata, T.; Pearson, D. S. *J. Rheol.* **1994**, *38*, 601.
(41) Bates, F. S. *Macromolecules* **1984**, *17*, 2607.
(42) Madbouly, S. A.; Ougizawa, T. *J. Macromol. Sci., Part B: Phys.* **2002**, *41*, 271.
(43) Kapnistos, M.; Hinrichs, A.; Vlassopoulos, D.; Anastasiadis, S. H.; Stammer, A.; Wolf, B. A. *Macromolecules* **1996**, *29*, 7155.
(44) Sato, T.; Watanabe, H.; Osaki, K. *Macromolecules* **2000**, *33*, 1686.
(45) Zhao, Y.; Cao, Y.; Yang, Y.; Wu, C. *Macromolecules* **2003**, *36*, 855.
(46) Eckstein, A.; Suhm, J.; Friedrich, C.; Maier, R. D.; Sassmannshausen, J.; Bochmann, M.; Mulhaupt, R. *Macromolecules* **1998**, *31*, 1335.
(47) Segre, P. N.; Prasad, V.; Schufield, A. B.; Weitz, D. A. *Phys. Rev. Lett.* **2001**, *86*, 6042.

MA050453U